This is an electronic version (author's version) of the paper:

Marin P., Fissore D., Barresi A. A., Ordóñez S. (2009). Simulation of an industrial-scale process for the SCR of NOx based on the loop reactor concept. Chemical Engineering & Processing: Process Intensification (Elsevier), 48(1), 311-320. DOI: 10.1016/j.cep.2008.04.008.

Simulation of an industrial-scale process for the SCR of NO_x based on the loop reactor concept

Pablo Marín[1,2], Davide Fissore[*,2], Antonello A. Barresi[2], Salvador Ordóñez[1]

(1) Department of Chemical Engineering and Environmental Technology, University of Oviedo, Facultad de Química, Julián Clavería 8, Oviedo, 33006, Spain

(2) Dipartimento di Scienza dei Materiali e Ingegneria Chimica, Politecnico di Torino, C.so Duca degli Abruzzi 24, Torino, 10129, Italy

[*] Corresponding author:
e-mail: davide.fissore@polito.it
Tel: +39-011-5644695
Fax: +39-011-5644699

Abstract

This paper investigates the possibility of using an adiabatic loop reactor to carry out the Selective Catalytic Reduction of NO_x with NH_3. The advantages of this technology with respect to more traditional reactors operated in steady-state are discussed: when the temperature of the feed is low, a lower amount of heat is required to get full NO_x conversion; moreover, the catalyst can be used to store a high amount of NH_3 during the operation, thus preventing NH_3 slip and/or NO_x emissions when the feed composition changes. Both issues are investigated, using the design of an industrial-scale reactor as case study.

Keywords

- Selective Catalytic Reduction
- Unsteady-state reactor
- Loop Reactor
- Reactors Network
- Autothermal reactor

Introduction

This paper is focused on the results that can be achieved when the SCR of NO_x with NH_3 is carried out in a Loop Reactor (LR), a recent and potentially valuable technology that allows for multifunctional operation:

1. the catalyst (and, eventually, the inert present in the reactor) can be used as a heat storage device due to the possibility of trapping the heat of reaction inside the reactor, thus maintaining a high temperature level; this *regenerative heat recovery* is generally much more efficient than recuperative heat exchange. This feature allows, for example, the catalytic combustion of gaseous emissions containing organic pollutants at low concentration, strongly reducing the need of auxiliary fuel to sustain the reaction and thus reducing the CO_2 emissions (Brinkmann et al., 1999; Fissore and Barresi, 2002; Fissore et al., 2004; Fissore et al., 2005; Barresi et al. 2007). Also in the case of the SCR the LR can make possible auto-thermal operation in case of cold feed, or, at least, it can reduce significantly the energy consumption of the process.
2. The catalyst can be also used to achieve *chromatographic separation*, i.e. the coupling between chemical reaction and adsorptive separation, if the solid is an adsorbent which has a high adsorption capacity toward a reactant and a low one toward a product, so that the strongly adsorbed reactant is trapped inside the reactor. The SCR of NO_x with NH_3 can take large advantage from this mode of reactor operation in presence of a catalyst that adsorbs NH_3 (Botar-Jid et al., 2005; Fissore et al. 2006a, 2006b, 2006c).

The Network of Reactors (RN) with periodical movement of the feeding position from one reactor to the following one of the sequence is one of the simplest ways to realise a LR (Figure 1A): a set of valves allows to change the feeding position, thus simulating the behaviour of a moving bed and achieving a sustained dynamic behaviour. A network of three reactors is studied in this

work: acting on a set of valves it is possible to change periodically the sequence of the reactors from the initial 1-2-3 to 2-3-1 and finally to 3-1-2 (Figure 1B).

An alternative device which allows for similar results is the Reverse Flow Reactor (RFR), a system where the sustained dynamic behaviour is obtained by periodically reversing the flow direction. The RFR has a serious drawback, namely the wash-out, i.e. the emission of unconverted reactants occurring when the flow direction is reversed. In the LR (and thus in the RN) the gas flow direction is never reversed, thus preventing any wash-out, but the range of operating variables giving stable and auto-thermal operation is narrower than in the RFR, thus requiring a much more efficient control system to ensure the full conversion of the reactants, in particular when the inlet flow rate and/or the feed composition is highly variable with time (Fissore et al., 2004).

Various issues concerning the SCR of NO_x carried out in a RN have been investigated in the past by our Research Group. A simple one-dimensional model was used to investigate theoretically the feasibility of the process (Botar-Jid et al, 2005; Fissore et al., 2006a), while a simplified model was used to carry out the bifurcational analysis in order to point out the influence of the operating parameters and of the kinetic activity of the catalyst on the performance of the system (Fissore et al., 2006b). A first attempt to validate the results obtained by means of mathematical simulation was that of Fissore et al. (2006c), who realised a lab-scale RN working at constant temperature. The aim of this paper is to investigate the problem of the design of an industrial scale RN for the SCR of NO_x with NH_3. Firstly, the procedure required for the process development is given, briefly analysing some issues concerning the investigation of the catalyst and the modelling and design of the equipment and of the process. In fact, in order to achieve an optimal design of this reactor, it is of outmost importance to know the kinetics of the reactions involved and it is important to use a

mathematical model to investigate the influence of the parameters of the system. A test case will be shown as an example of the design of the process.

Process development

Various steps are required to design the process: firstly the catalyst has to be fully characterised with respect to the reaction kinetics; then, the reactor configuration has to be selected, by analysing if auto-thermal behaviour can be achieved or if additional heat has to be supplied to the device. Finally, the operation of the reactor has to be investigated in order to select the values of the main operating parameters.

Catalyst characterisation

The role of the catalyst in the process of SCR of NO_x in the RN has been investigated by Fissore et al. (2006b); using a very simplified model of the process and the bifurcational analysis, they pointed out the optimal values of the kinetic properties of the catalyst that can guarantee stable operation with full reactants conversion without external energy supply. They also evidenced that the adsorption capacity can play a role even more important than the catalytic activity. Beside this, also the thermal properties of the catalyst (namely the heat capacity and the heat conductivity) play an important role, as they are responsible of the storage of the heat of reaction, as it has been pointed out by Fissore and Barresi (2003) in the case of a RFR where the treatment of gaseous streams containing organic pollutants at low concentration is carried out. The optimal values of the properties of the catalyst can be different from those of the catalyst designed for steady-state reactors. Anyway, in this paper we assume to use a commercial honeycomb catalyst for the process as it is not easy at all to

modify the catalytic activity or the adsorption capacity of a catalyst of various orders of magnitude as it should be necessary, according to previous results (Fissore et al., 2006b). The kinetic parameters of the adsorption, desorption and reduction reactions, as well as the catalyst capacity, can be evaluated by means of experiments, using transient methods consisting of imposing perturbations to the reacting system (e.g. changes of the inlet reactant concentration or of the catalyst temperature) while continuously monitoring the outlet response (Kobayashi and Kobayashi, 1974; Lietti et al., 1997, 1998). By imposing step-wise changes in the inlet NO and/or NH_3 concentration, the dynamics of the SCR reaction can thus be investigated and the adsorption/desorption of the reactants can be investigated separately from their surface reaction, thus gaining detailed information on each step of the reaction. Quantitative indications about the kinetics of the reactions are obtained by analysing these results according to the dynamic model of the reacting system (Lietti et al., 1997): to this purpose, a one-dimensional heterogeneous model has been used; the main features of the model are the followings:

1. NO reacts from the gas phase with strongly adsorbed (and activated) ammonia molecules (Odenbrand et al., 1994; Inomata et al., 1980); thus, an Eley-Rideal mechanism is used to describe the reaction between NO (A) in the gas phase and the ammonia (B) adsorbed on the catalyst;
2. O_2, which is required by the SCR reaction:

   $$4\,NO + 4\,NH_3 + O_2 \rightarrow 4\,N_2 + 6\,H_2O \qquad (1)$$

   is considered to be in great excess and, thus, its concentration is assumed to remain constant during the operation;
3. the reduction reaction is considered to be of first order with respect to each reactant;
4. the rate of adsorption of ammonia on the catalyst surface is assumed to be

proportional to the ammonia concentration in the gas phase and to the free fraction of surface sites, while the rate of desorption is assumed to be proportional to the concentration of the adsorbed ammonia;

5. an Arrhenius-type dependence of the kinetic constants k_{red}, k_{ads} and k_{des} from the temperature is assumed;
6. a Temkin-type desorption kinetics is assumed; thus, the activation energy for desorption is a function of the surface coverage.

Table 1 summarises the equations used to describe the kinetic of the reactions of adsorption/desorption of NH_3 and of reduction of NO_x.

The process dynamics in the reactor is described by the mass balance for the gas and for the solid phases, as the kinetic study is generally carried out at constant temperature (see, for example, Fissore et al. 2006a, where details about the parameters of the model and about the numerical solution of the equations are given).

Reactor configuration

A simple calculation can be carried out to check if the SCR reaction can be carried out auto-thermally in the RN: if ΔT_p is the pre-heating temperature rise required to carry the feed to the working temperature of the reactor and ΔT_{ad} is the adiabatic temperature rise of the feed, given by:

$$\Delta T_{ad} = \frac{c_{feed}\left(-\Delta H\right)}{\rho c_p} \tag{2}$$

auto-thermal operation is possible only if the required pre-heating (Q_{ph}) is lower than the heat that can be recovered (Q_r), where:

$$Q_{ph} = \dot{V}\rho c_p \Delta T_p \tag{3}$$

$$Q_r = \eta\left[\dot{V} c_{feed}\left(-\Delta H\right) + \dot{V}\rho c_p \Delta T_p\right] \tag{4}$$

being η the heat recovery efficiency, ρc_p a mean value of heat capacity in the

range ΔT_p and assuming full reactant conversion. Thus, $Q_{ph} < Q_r$ implies that:

$$\Delta T_p < \eta\left(\Delta T_{ad} + \Delta T_p\right) \tag{5}$$

By rearranging eq. (5) we obtain that auto-thermal operation is possible if:

$$\Delta T_{ad} > \Delta T_p \frac{1-\eta}{\eta} \tag{6}$$

i.e. the ΔT_{ad} of the feed should be higher than ΔT_p multiplied by a number which is a function of the heat recovery efficiency. Figure 2 shows various lines corresponding to eq. (6) with various values of η: for a certain process auto-thermal behaviour is possible only if the couple of values (ΔT_{ad} ,ΔT_p) lays above the line corresponding to the heat recovery efficiency that can be achieved. The value of ΔT_{ad} is a function of the feed concentration, while the ΔT_p depends on the temperature of the feed and on the catalyst used. If auto-thermal operation is not possible, some heat must be supplied to the system. As a first guess, the curve corresponding to η = 70% can be considered representative of a system where recuperative heat exchange takes place, while the curve calculated for η = 90-95% is representative of a process with regenerative heat recovery, as it happens in the RN; thus, for the couples of values (ΔT_{ad}, ΔT_p) laying in the portion of the graph between these two curves auto-thermal operation can be achieved, but only in presence of regenerative heat recovery. If the point corresponding to the process falls below the curve calculated for η = 95% an energy input is required to carry out the reaction, but it is lower in case of regenerative heat recovery. Obviously, these numbers have to be considered as a rough estimate of the heat recovery efficiency that is obtained in the real apparatus; as a consequence, it may happen that even if auto-thermal operation can be expected in the RN according to the curves of Figure 2, assuming for the heat recovery efficiency a value close to the highest range, the mathematical simulation of the whole process finally points out that some heat is anyway

required to sustain the reaction: in this case the design of the system should be modified in order to reach a higher value of heat recovery efficiency. The diagram of Figure 2 has been calculated for adiabatic operation, as it is generally the case of industrial-scale apparatus; in case of heat loss, this term can be easily subtracted from eq. (4) as this heat is not recovered in any device: the result is a reduction of the heat recovery efficiency.

If a heat supply is required, even in presence of regenerative heat recovery, i.e. using the RN, three different strategies can be considered. In the first strategy all the heat is supplied by an electrical heater placed after the first reactor of the network. Due to the periodical movement of the feeding position, one reactor can be the first of the sequence during a phase of the operation and the second, or the third, of the sequence in the successive steps; thus, three electrical heaters are required, one after each reactor and, in this first strategy, only the heater after the first reactor of the sequence is switched on. In the second strategy all the heat is supplied by the heater placed after the second reactor of the sequence. In the third strategy two heaters are switched on, those after the first and after the second reactor of the sequence. These arrangements are not the only ones that can be designed to supply energy (heat) to the system, but they are surely the simplest to be realised.

Equipment modelling

A mathematical model is required to simulate the dynamics of the process in order to find the value of the operating parameters (e.g. the switching time) that allow for auto-thermal operation or, in case this is not achievable, the minimum amount of heat that has to be supplied to the system in order to sustain the reaction. A one-dimensional model can be adequate to this purpose, assuming also that pressure loss is negligible and that the reactor is adiabatic, as it is

generally the case of industrial-scale units; if heat loss is relevant, this can be taken into account in the energy balance of the system (Barresi et al., 1999). The system of partial differential equations that describes the process dynamics in the reactor is given in Table 2: it is possible to see that heat losses due to the heat exchange with the external environment are accounted for; a more rigorous approach would consists of taking into account the heat balance of the reactor wall and modelling these heat losses as occurring between the wall and the external environment (Fissore et al., 2005). The value of $c_{A,i}$ and $c_{B,i}$, the gas concentration at the interface, can be calculated from the mass balance at the interface, assuming that there is no accumulation at the catalyst-gas interface. Inlet composition of the gas is considered equal to the feeding value. The origin of the x-axis corresponds to the inlet section to the network; consequently it translates from the first reactor of the sequence to the second one when the switching time is reached. At this point the boundary conditions are switched in order to simulate the variation of the feeding position. The adequacy of this model to describe the RN has been demonstrated in a previous paper (Fissore et al., 2006c) using a lab-scale apparatus, but, as the model is based on first principles, it can be used also to describe the dynamics of equipment having a larger size. Further tests have been carried out in this work on the same lab-scale apparatus, investigating a larger interval of operating conditions. All the tests have been carried out operating under isothermal conditions and using a RN of three reactors operated at different temperatures, feed flow rates and compositions. All the reactors of the network contains the same amount of catalyst (each monolith is $5 \cdot 10^{-2}$ m long, no inert monoliths are used) and are placed in an oven to ensure a uniform temperature; five three-way valves are required to change the feeding position along the sequence of the three reactors. Experimental values are always compared with modelling predictions obtained

using the parameters of Table 3 and setting the values of the operating variables (temperature, flow rate, inlet concentration, switching time) to those used in the experimental run. Before start feeding NO, the catalyst is saturated with NH_3. The evolution of the NH_3 outlet concentration is then monitored and compared for each test. An example of the results that can be obtained is shown in Figure 3, where the experimental data (symbols) are compared with the values obtained by means of mathematical simulations (solid lines) for two different working temperatures (250 and 300°C). The agreement between experimental values and modelling predictions is quite good, taking into account both the simplifications of the model and the range of uncertainty of the measure (upper and lower boundaries of ±20 ppmV around the measured value, corresponding to the estimated analyser precision, are evidenced).

Design of an industrial-scale reactor

Case study and preliminary design

The case study used for the calculations is the treatment of 5000 $Nm^3\ h^{-1}$ of air at 25°C containing 800 mg Nm^{-3} of NO (corresponding to 600 ppmV) and a stoichiometric amount of NH_3 (added as co-reactant), i.e. 450 mg Nm^{-3}; these concentrations result in a ΔT_{ad} of 8 K. These values are representative of the typical situation occurring when the off-gases from a coal-fired power plant are treated; in this case, in fact, the SO_2 removal causes a relevant decrease of the gas temperature, which can be close to 20-25°C before entering the SCR unit.

In order to ensure full NO_x conversion, the catalyst has to work at a proper temperature, which must be high enough to provide good activity, without reaching the value at which the reaction of oxidation of ammonia takes place.

Commercial catalysts have a typical operating temperature in the range 300–380°C (Beeckmann and Hegedus, 1991). If the couple of values (ΔT_{ad}, ΔT_p) corresponding to our case study is placed in the diagram of Figure 2, it can be seen that auto-thermal operation is not possible even in presence of a device that allows for a heat recovery efficiency of 95%, i.e. in the RN: auto-thermal operation can be obtained in the LR only if the feeding concentration of NO is at least 1800 mg Nm^{-3}, which is more than twice the amount of NO present in a typical coal power plant emission.

Let us give some figures about our case study where a catalyst with an operating temperature of 350°C is used: at least 620 kW are required to heat the feed to the working temperature without any heat recovery. This value can be reduced by using a heat exchanger external to the reactor in order to recover the (small) heat of reaction and the (high) sensible heat supplied to the feed (Figure 4). The cold gas enters a heat exchanger where it is pre-heated to 120°C (this requires about 180 kW); then, it enters the heat recovery device where it reaches the temperature required by the process, while the products of reaction are cooled to 130°C. This means that about 70% of the heat necessary to the process is recovered. In the case of regenerative heat exchange, which can be achieved in the RN, heat recovery is expected to reach even 95%, thus lowering the energy consumption of the process.

The first step in the design of a catalytic reactor is the selection of the GHSV. Generally, the manufacturer of the catalyst suggests a value for the GHSV: for the SCR reaction values in the range 2000–7000 h^{-1} are generally proposed (Beeckmann and Hegedus, 1991) in the case of isothermal operation. In the RN the temperature profile is moving during the operation and thus part of the catalyst is at high temperature and part is at low temperature; for this reason a higher amount of catalyst with respect to the traditional steady-state

process is required. A GHSV of 2000 h^{-1} is chosen as a starting value, so that the amount of catalyst required for the feed flow rate can be calculated. In order to determine the length and diameter of the reactor, a ratio of the length to diameter of 1:1 is assumed. This ratio is usually avoided in packed-bed reactors because such a low value can cause back-mixing and deviation from the plug flow. Nevertheless, when using honeycomb catalysts, as in the present work, due to the lower heat capacity with respect to that of a packed bed, low length to diameter ratios are preferred in order to get lower gas velocity, and thus lower velocity of the heat wave. Deviation from the plug flow is much more difficult because the gas flows in channels of the monolith (in laminar regime). A length and diameter of the reactor of 1.5 m have been calculated for our case study, thus resulting in a gas velocity of 0.78 m s^{-1}.

Catalyst investigation

The commercial zeolite based NOxCAT™ ETZ honeycomb catalyst (supplied by Engelhard) has been investigated for the process. The lab-scale apparatus previously described, with only one reactor connected and a proper amount of catalyst (the length of the monolith is $8 \cdot 10^{-2}$ m in this case), has been used to calculate the kinetic parameters of the reactions occurring in the system. The temperature of the catalyst was measured and controlled: this temperature can be varied up to a maximum value of 400°C; the range 200-380°C has been investigated; total flow rate can vary in the range 0-4 L min^{-1} (STP). The concentration of the products of reaction in the outlet stream is measured continuously using a quadrupole mass spectrometer; the analytical procedure and the apparatus have been described by Fissore et al. (2006c).

The transient NH_3 adsorption/desorption study was performed at various temperatures by imposing step-wise perturbations of the NH_3 inlet

concentration in flowing Ar, while maintaining the overall flow rate constant. The whole set of experimental data has been analysed according to the previously described mathematical model. The MATLab routine FMINSEARCH, which implements a simplex method (Lagarias et al., 1998), has been used to calculate the kinetic parameters that allows for the best fit between the calculated and the experimentally measured values of concentration. The study of the reduction reaction has been carried out in a similar way as the adsorption/desorption study previously described: the catalyst bed has been firstly saturated with NH_3 and then the reactants have been fed into the reactor; the evolution of the composition of the gas leaving the reactor has been measured and the kinetic parameters of the reduction reaction have been calculated by best fitting with the experimental results. A similar investigation was performed in the past by Fissore et al. (2006c), but in a narrower range of operating conditions. Table 3 summarises the kinetic parameters calculated from all the experimental tests, together with the main physical properties of the catalyst.

Full plant design

As far as the design of the industrial-scale reactor is concerned, an external heat supply is required for the case study under investigation, as it has been previously pointed out. Figure 5 shows an example of the results that can be obtained using the previously described heating strategies: in the upper graph the conversion of NO as a function of the total amount of heat supplied to the system is shown, while in the lower graph the maximum temperature on the solid is given; the switching time is constant and equal to 60 s. It is possible to see that when all the heat is supplied only after the first reactor of the sequence an almost complete conversion of NO is obtained using about 65 kW, that

corresponds to an heat recovery of about 90%; for lower values of Q_{el} the conversion is lower, as well as for higher values (the conversion is calculated as the mean value over a cycle, when the periodic steady-state is reached). If all the heat is supplied after the second reactor of the sequence similar results are obtained: the maximum temperature of the catalyst is almost identical to the previous case, but the amount of heat required to guarantee full conversion is slightly higher, due to the different temperature profiles that are obtained in the reactor. Finally, a third configuration has been analysed, with part of the heat supplied by the first heater (one half of the total) and part by the second heater. This case seems to be less efficient because, even if the full conversion of NO is guaranteed for a larger interval of Q_{el}, higher amount of heat are required with respect to the first configuration; this is due to the lower temperature level in the reactor, as it can be seen from the values of maximum temperature of the catalyst obtained in this case (see Figure 7 and 8): the temperature profile established in the reactors is in fact responsible of the total conversion obtained.

Figure 6 shows the role of the switching time on the total NO conversion when 65 kW are supplied after the first reactor of the sequence. The results show that it is possible to find an optimum in the value of the switching time in order to maximise the conversion of the reactants. This is in agreement with the results given in the Literature for other processes carried out in the RN, where it was shown that a narrow interval of switching time was required to ensure full reactant conversion. It is important to highlight that the value of the amount of heat that is required to guarantee the auto-thermal behaviour has to be calculated by means of detailed simulations of the reactor as the dynamics of the system strongly affects the heat storage capacity of the system. Figure 6 shows also the values of heat recovery efficiency obtained in the system as a function of the switching time, pointing out that values around 90% are

obtained, with a maximum in correspondence of the maximum conversion of NO.

The axial profiles of temperature, gas phase concentration and ammonia surface coverage given in Figure 7 and 8 helps to explain the results of Figure 5 and 6. These profiles are those obtained at the end of a cycle, once the periodic steady-state is reached. Figure 7 evidences that, for a fixed value of the switching time, increasing the value of Q_{el} from 50 kW to 65 kW increases the values of the temperature in the reactor and this reduces the surface coverage (due to the higher desorption rate), but the positive effect of increasing the reduction rate prevails, resulting in a net increasing of NO conversion. If Q_{el} is further increased to 90 kW the negative effect of the desorption of ammonia (evidenced by a lower surface coverage) is prevailing, thus decreasing the NO conversion.

A similar behaviour can be seen when the switching time is varied (Figure 8): moving from 20 s, to 50 s and then to 80 s the temperature profile is strongly affected in a non-monotonic way, thus resulting in different values of the ammonia concentration in the gas phase and on the solid surface, resulting in the curves shown in Figure 6.

When the reactor has been designed and the operating parameters (Q_{el}, t_c) have been selected, it is worthwile to analyse the behaviour of the system doring the start-up. This is shown in Figure 9 for a RN operated with a switching time of 60 s and with 65 kW supplied after the first reactor of the network. It is possible to see that after about 1 h the temperature of the product stream reaches its final value, while about 3 h are required to get the final value of the conversion of NO; in the Figure it is shown also the mean surface coverage of the NH_3 in the reactor in order to confirm that the true pseudo-steady state has been reached. With respect to the heat losses, a value of the

heat exchange coefficient between the reactor and the external environment equal to 0.18 W $m^{-2}K^{-1}$ has been assumed, in order to evaluate the possible relevance of heat losses and their effect on the behaviour of the reactor, this results in a mean value of heat losses of about 0.5 kW, a value that has no effect on the temperature profile and on the thermal balance of the system (this result does not change significantly in presence of higher values of heat exchange coefficient as well as in the other operating conditions tested).

Finally, the whole procedure that has been used to design the industrial scale RN is summarised in Figure 10, where it is pointed out that if the mathematical simulation of the equipment indicates that the emissions of NO_x and/or that of NH_3 are above the emission limits, some of the decisions taken during the design procedure have to be modified, namely:

- the switching time can be reduced up the minimum feasible value;
- the heat supply can be increased (up to a maximum value that makes this process no more profitable with respect to the fixed bed with recuperative heat exchanger);
- the reactor length to diameter ratio can be decreased, thus using lower gas velocity (up to a limit that causes problems with the gas distribution);
- the GHSV can be decreased, thus using a higher amount of catalyst (also in this case, up to a maximum amount of catalyst that makes this process no more profitable with respect to the traditional technology).

Finally, when a reactor design that ensures the fulfilment of the emission limits has been obtained, a further optimisation can be carried out, aiming to increase the heat recovery efficient if the value obtained is below the target of 90-95%. This means to try to lower the value of heat supplied and then repeating the design procedure described above (thus acting on the switching time, on the reactor length to diameter ratio and on the GHSV).

Response to disturbances

Finally, the response of the system to changes in the feed concentration can also be investigated in order to point out the process applicability. For this purpose two different cases have been investigated: in the first, the feeding of NO is stopped, while, in the second, the feeding of NH_3 is stopped (the reactor is assumed to be initially at the periodic steady-state obtained with a switching time of 60 s and 65 kW supplied to the gas by the heater placed after the first reactor of the sequence). Results are given in Figure 11: when the feeding of NO is stopped, the NH_3 is initially adsorbed on the catalyst; at the same time, the temperature of the catalyst starts decreasing as the reduction reaction does not take place any more. After about one hour (Figure 11, upper graph) the conversion of NH_3 becomes zero due to the simultaneous effect of the low temperature and of the saturation of the catalyst. This way, the RN configuration is able to overcome perturbations in the concentration of NO, avoiding emissions of unreacted NH_3 for longer time than in the traditional fixed-bed SCR process. This is one of the most important advantages of the RN. When the NH_3 feed is stopped, the NO can react with the NH_3 adsorbed on the catalyst surface and the conversion starts decreasing slowly and becomes zero only when no further NH_3 is available for the reduction reaction.

Conclusions

The possibility of using an industrial-scale RN to carry out the SCR of NO_x with NH_3 has been investigated in this paper. A case study representative of this process has been selected and the advantages that can be achieved in the RN have been highlighted, namely a strong reduction of the energy requirement (65

kW vs. 130 kW) and the avoidance of any NH_3 slip due to the flow path. The main drawback is represented by the reactor configuration, whose piping is much more "complex" than in the traditional system, but fixed capital savings can be obtained as the large (because of the low heat transfer coefficient) and expensive heat exchanger used to recover heat from the reactor products is no more required, and it is substituted by a couple of simple electric heaters.

Moreover, a further advantage that can be achieved, i.e. the possibility of operating properly in presence of feed with variable concentration, has been pointed out by means of mathematical simulation.

The whole procedure that should be used to design this kind of reactor has been given and the influence of the main operating parameters (heating required, switching time) has been investigated, thus providing some general guidelines for the design.

Acknowledgements

Pablo Marin is grateful to the Spanish Ministry of Education for the PhD grant that supports his research and his stage at the Politecnico of Torino, during which the experimental study was carried out.

Notation

A, B	reactants
a_e	external surface of the reactor per unit of volume, m^{-1}
a_v	specific surface of the catalyst, m^{-1}
c	concentration, mol m^{-3}
c_p	specific heat, J kg^{-1} K^{-1}
D_h	hydraulyc diameter of the channels of the monolith, m
E_a	activation energy, J mol^{-1}
h_e	heat transfer coefficient between the gas and the external environment, J m^{-2} K^{-1} s^{-1}
h_T	heat transfer coefficient between the gas and the solid, J m^{-2} K^{-1} s^{-1}
ΔH	heat of reaction, J mol^{-1}
k	kinetic constant
kc	mass transfer coefficient, m s^{-1}
k_0	frequency factor
l	length of each reactor of the network
$\dot{m}$	flow rate, kg s^{-1}
Q_{el}	heat supplied by the electrical heater, kW
Q_{ph}	heat required to pre-heat the feed, W
Q_r	recovered heat, W
r	rate of reaction, mol s^{-1} m^{-3}
R	gas constant, J K^{-1} mol^{-1}
t	time, s
t_C	switching time, s
T	temperature, K
x	axial coordinate, m
v	gas velocity, m s^{-1}

$\dot{V}$	volumetric flow rate, $m^3\ s^{-1}$

Greeks

β	parameter for the surface coverage dependence
ε	porosity of the monolith
ΔH	variation of enthalpy, $J\ mol^{-1}$
ΔT_{ad}	adiabatic temperature rise, °C
ΔT_p	pre-heating temperature rise, °C
η	heat recovery efficiency
θ	surface coverage
ρ	density, $kg\ m^{-3}$
σ, ζ	parameters for the surface coverage dependence
Ω	catalyst capacity, $mol\ m^{-3}$

Subscripts and Superscripts.

ads	adsorption
des	desorption
e	external
feed	feeding value
G	gas phase
i	value at the gas-solid interface
j	*j*-th reacting species
max	maximum value
red	reduction
S	solid phase

Abbreviations

GHSV	Gas Hourly Space Velocity , h^{-1}
LR	Loop Reactor
RFR	Reverse Flow Reactor
RN	Reactors Network
SCR	Selective Catalytic Reduction
STP	Standard Temperature and Pressure

References

Barresi A. A., Vanni M., Brinkmann M., Baldi G. (1999). Influence of the wall heat losses on the performance of a network of nonstationary catalytic burners. Chemical Engineering & Technology, 22(3), 237-239.

Barresi A. A., Baldi G., Fissore D. (2007). Forced unsteady-state reactors as efficient devices for integrated processes: case histories and new perspectives. Industrial Engineering & Chemistry Research, 46, 8693-8700.

Beeckmann, J. W., Hegedus, L. L. (1991). Design of monoliths catalysts for power plant NO_x emission control. Industrial Engineering Chemistry Research, 30, 969–978.

Botar-Jid, C. C., Agachi, P. S., Fissore, D., Barresi, A. A. (2005). Selective Catalytic Reduction of NO_x with NH_3 in unsteady-state reactors. Studia Universitatis Babes-Bolyai: Chemia, 50, 29-40.

Brinkmann, M., Barresi, A. A., Vanni, M., Baldi, G. (1999). Unsteady-state treatment of very lean waste gases in a network of catalytic burners. Catalysis Today, 47, 263-277.

Fissore, D., Barresi, A. A. (2002). Comparison between the reverse-flow reactor and a network of reactors for the oxidation of lean VOC mixtures. Chemical Engineering and Technology, 25, 421-426.

Fissore D., Barresi A. A. (2003). On the influence of the physical properties of the catalyst on the performances of forced unsteady-state after-burners. Chemical Engineering Research & Design, 81, 611-617.

Fissore, D., Barresi, A. A., Velardi, S., Vanni, M. (2004). On the properties of the forced unsteady-state ring reactor network. Chinese Journal of Chemical Engineering, 12, 408-414.

Fissore D., Barresi A. A., Baldi G., Hevia M. A. G., Ordóñez S., Díez F. V. (2005).

Design and testing of small scale unsteady-state afterburners and reactors. AIChE Journal, 51, 1654-1664.

Fissore, D., Barresi, A. A., Botar-Jid, C. C. (2006a). NO_x removal in forced unsteady-state chromatographic reactors. Chemical Engineering Science, 61, 3409-3414.

Fissore, D., Penciu, O. M., Barresi, A. A. (2006b). SCR of NO_x in loop reactors: asymptotic models and bifurcational analysis. Chemical Engineering Journal, 122, 175-182.

Fissore, D., Garran, D., Barresi, A. A. (2006c). Experimental investigation of the SCR of NO_x in a Simulated Moving Bed Reactor. AIChE Journal, 52(9), 3146-3154.

Inomata, M., Miyamoto, A., Toshiaki, U., Kobayashi, K., Murakami, Y. (1980). Mechanism of the reaction of NO and NH_3 on vanadium oxide catalyst in the presence of oxygen under the dilute gas condition. Journal of Catalysis, 62, 140-148.

Kobayashi, H., Kobayashi, M. (1974). Transient response method in heterogeneous catalysis. Catalysis Review-Science and Engineering, 10, 139-146.

Lagarias, J. C., Reeds, J. A., Wright, M. H., Wright, P. E. (1998). Convergence properties of the Nelder-Mead simplex method in low dimensions. SIAM Journal of Optimization, 9, 112-147.

Lietti, L., Nova, I., Camurri, S., Tronconi, E., Forzatti, P. (1997). Dynamics of the SCR-$DeNO_x$ reaction by the transient-response method. AIChE Journal, 43, 2559-2570.

Lietti, L., Nova, I., Tronconi, E., Forzatti, P. (1998). Transient kinetic study of the SCR-$DeNO_x$ reaction. Catalysis Today, 45, 85-92.

Odenbrand, C. U. I., Bahamonde, A., Avila, P., Blanco, J. (1994). Kinetic study of

the selective reduction of nitric oxide over vanadia-tungsta-titania/sepiolite catalyst. Applied Catalysis B: Environmental, 5, 117-131.

List of Tables

List of Figures

Solid line: all the heat is supplied by the heater placed after the first reactor in the sequence; dashed line: all the heat is supplied by the heater placed after the second reactor in the sequence; dotted line: the same amount of the heat (equal to one half of the total) is supplied by the two heaters (switching time: 60 s).

Figure 6 Dependence of the conversion of NO (squares) and of the heat recovery efficiency (circles) on the switching time. 65 kW are supplied by the heater placed after the first reactor in the sequence.

Figure 7 Comparison between the axial profiles of the gas temperature (graph A), of the ammonia gas-phase concentration (graph B) and of the ammonia surface coverage (graph C) for various amount of heat supplied by the heater placed after the first reactor in the sequence. Solid line: 50 kW; dashed line: 65 kW; dotted line: 90 kW (switching time: 60 s).

Figure 8 Dependence of the axial profiles of the gas temperature (graph A), of the ammonia gas-phase concentration (graph B) and of the ammonia surface coverage (graph C) on various values of the switching time. Solid line: 20 s; dashed line: 50 s; dotted line: 80 s (heat supplied: 60 kW after the first reactor).

Figure 9 Mean temperature of the gas product (Δ), of the conversion of NO (o) and of the ammonia surface coverage (□) during the start-up of the reactor when t_c = 60 s (heat supplied: 65 kW after

the first reactor).

Figure 11 Chart describing the whole design procedure of the RN (rectangular boxes: operating parameters; circles: design variables). Some of the values used for the case study are indicated.

Figure 12 Upper graph: Time evolution of the NH_3 concentration in the product stream when the feeding of NO is stopped.
Lower graph: Time evolution of the NO concentration in the product stream when the feeding of NH_3 is stopped.
(switching time: 60 s, heat supplied: 65 kW after the first reactor).

Table 1

Reduction of NO_x with NH_3	$r_{red} = -k_{red} c_{A,i} \theta_B \Omega$	$k_{red} = k_{0,red} e^{-E_{a,red}/RT_S}$
Adsorption of NH_3 onto the catalyst surface	$r_{ads} = k_{ads} c_{B,i} \left(1-\theta_B\right) \Omega$	$k_{ads} = k_{0,ads}{}^{-E_{a,ads}/RT_S}$
Desorption of NH_3 from the catalyst	$r_{des} = k_{des} \theta_B \Omega$	$k_{des} = k_{0,des} e^{-E_{a,des}/RT_S}$ $E_{a,des} = E_{a,des}^{\zeta} \left(1-\beta \theta_B{}^{\sigma}\right)$

Table 2

Gas phase mass balances	$\frac{\partial c_A}{\partial t} = -v\frac{\partial c_A}{\partial x} + k_{c,A}a_v\left(c_{A,i} - c_A\right)$ $\frac{\partial c_B}{\partial t} = -v\frac{\partial c_B}{\partial x} + k_{c,B}a_v\left(c_{B,i} - c_B\right)$
Solid phase mass balance	$\Omega\frac{\partial \theta_B}{\partial t} = r_{ads} - r_{des} - r_{red}$
Gas phase energy balance	$\frac{\partial T_G}{\partial t} = -v\frac{\partial T_G}{\partial x} - \frac{h_T a_v}{\rho_G c_{p,G}}\left(T_G - T_S\right) - \frac{h_e a_e}{\rho_G c_{p,G}}\left(T_G - T_e\right)$
Solid phase energy balance	$\rho_S c_{p,S}\left(1-\varepsilon\right)\frac{\partial T_S}{\partial t} = -h_T a_v\left(T_S - T_G\right) + r_{red}\left(-\Delta H_{red}\right) + + r_{ads}\left(-\Delta H_{ads}\right) + r_{des}\left(-\Delta H_{des}\right)$
Mass balances at the interface	$-k_{c,A}a_v\left(c_{A,i} - c_A\right) = r_{red}$ $-k_{c,B}a_v\left(c_{B,i} - c_B\right) = \left(r_{ads} - r_{des}\right)$
Switching conditions	$x \in]0, 2\ell[\quad \begin{cases} c_j(x)\big\|_{t^+} = c_j(x+\ell)\big\|_{t^-} \\ T_G(x)\big\|_{t^+} = T_G(x+\ell)\big\|_{t^-} \\ T_S(x)\big\|_{t^+} = T_S(x+\ell)\big\|_{t^-} \end{cases}$ $x \in [2\ell, 3\ell] \quad \begin{cases} c_j(x)\big\|_{t^+} = c_j(x-2\ell)\big\|_{t^-} \\ T_G(x)\big\|_{t^+} = T_G(x-2\ell)\big\|_{t^-} \\ T_S(x)\big\|_{t^+} = T_S(x-2\ell)\big\|_{t^-} \end{cases}$

Table 3

$k_{0,ads}$, $m^3\ mol^{-1}\ s^{-1}$	0.84 ± 0.16
$E_{a,ads}$, $J\ mol^{-1}$	0
$k_{0,des}$, s^{-1}	$(9 \pm 1) \cdot 10^5$
$E^{\zeta}_{a,des}$, $J\ mol^{-1}$	$(109 \pm 6) \cdot 10^3$
β	0.11 ± 0.05
σ	1
$k_{0,red}$, s^{-1}	$(1.2 \pm 0.1) \cdot 10^5$
$E_{a,red}$, $J\ mol^{-1}$	$(60 \pm 2) \cdot 10^3$
ε	0.75
D_h	$2.54 \cdot 10^{-3}$ m
ρ_S	2500 $kg\ m^{-3}$
$c_{p,S}$	900 $J\ kg^{-1}\ K^{-1}$

Figure 1

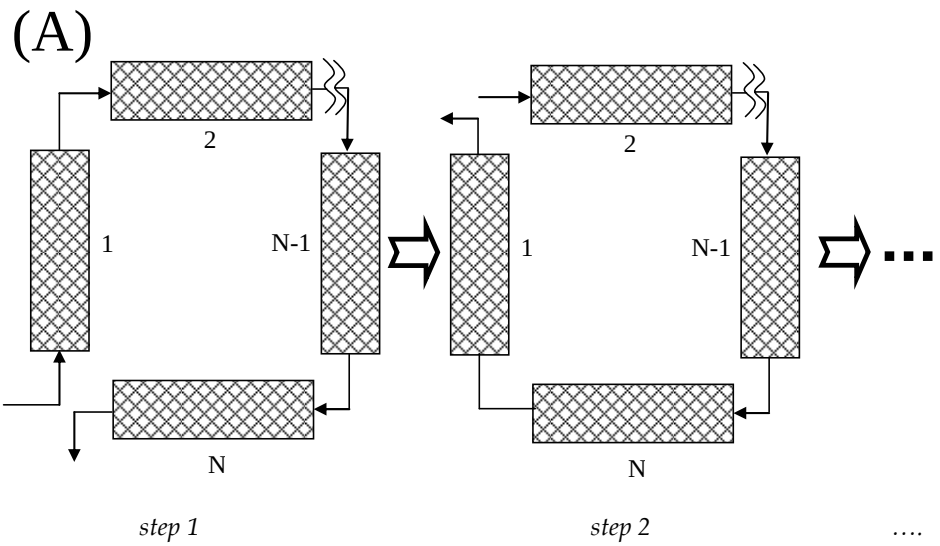

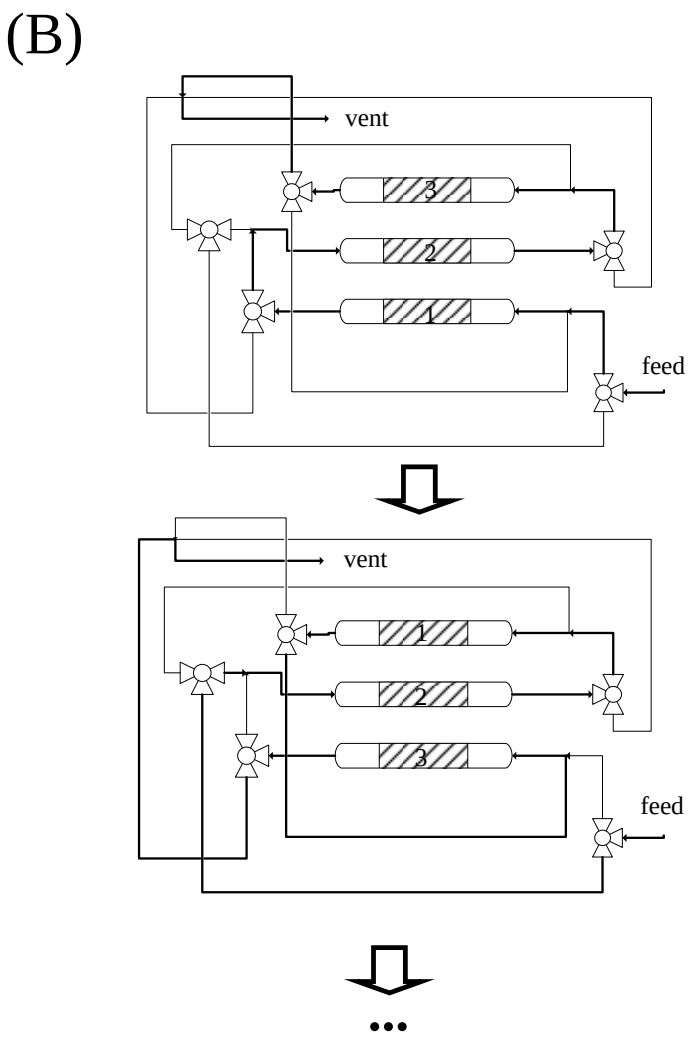

Figure 2

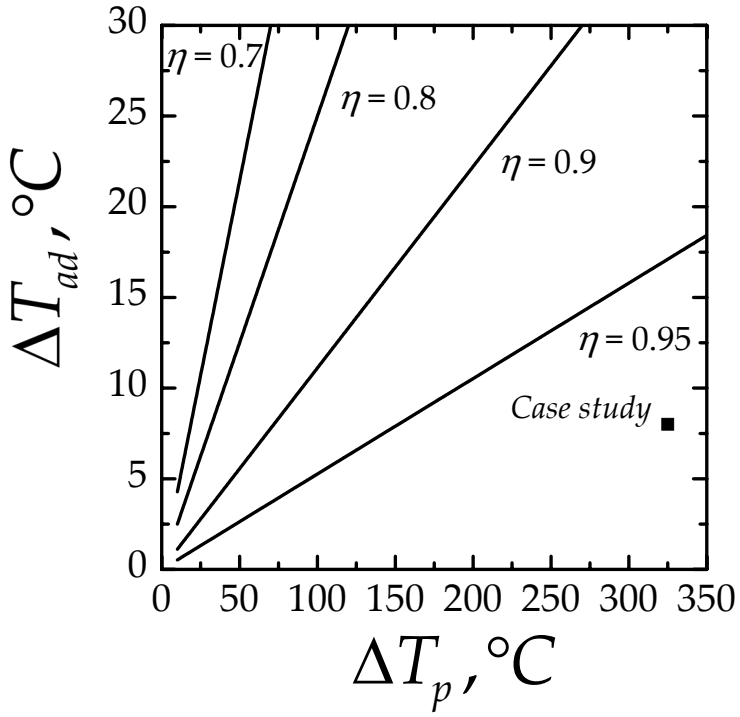
30
25
20
15
10
5
0
0
50
100
150
200
250
300
350
η = 0.7
η = 0.8
η = 0.9
η = 0.95
Case study
ΔT_{ad}, °C
ΔT_p, °C

Figure 3

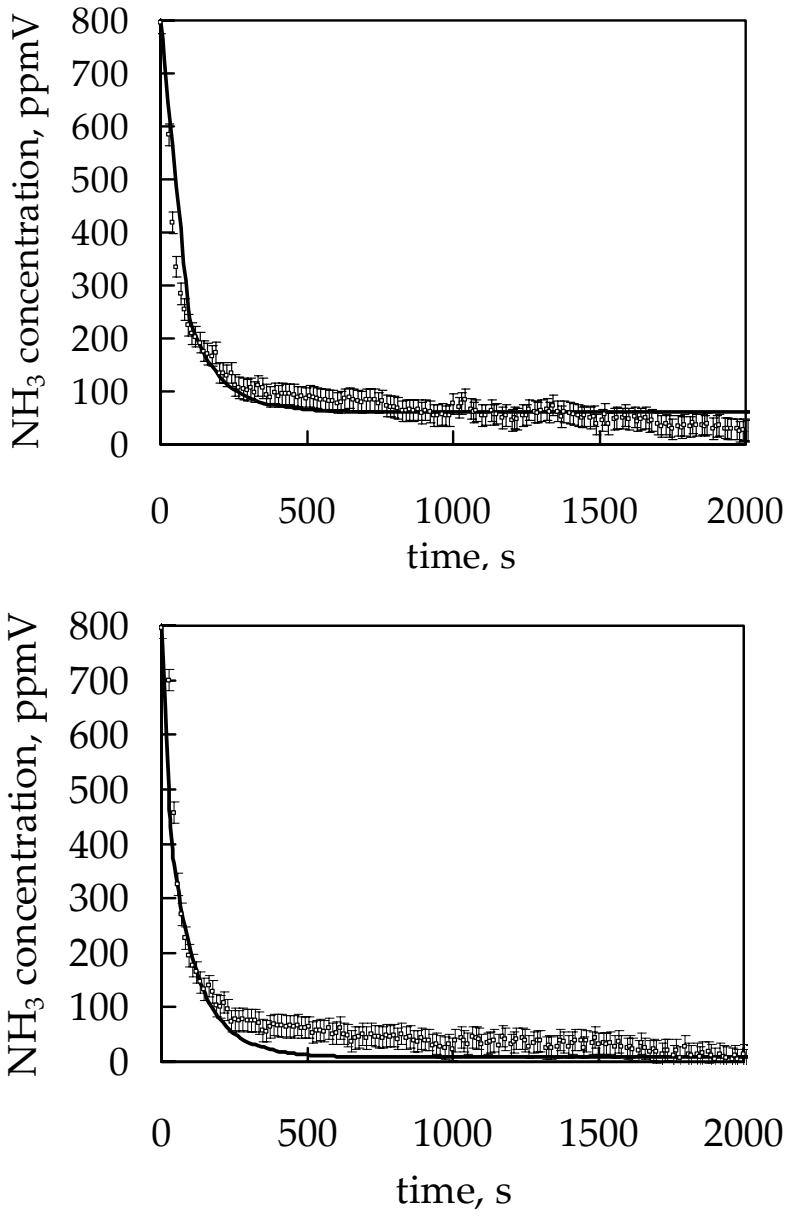
800
700
600
500
400
300
200
100
0
NH3 concentration, ppmV
0
500
1000
1500
2000
time, s
800
700
600
500
400
300
200
100
0
NH3 concentration, ppmV
0
500
1000
1500
2000
time, s

Figure 4

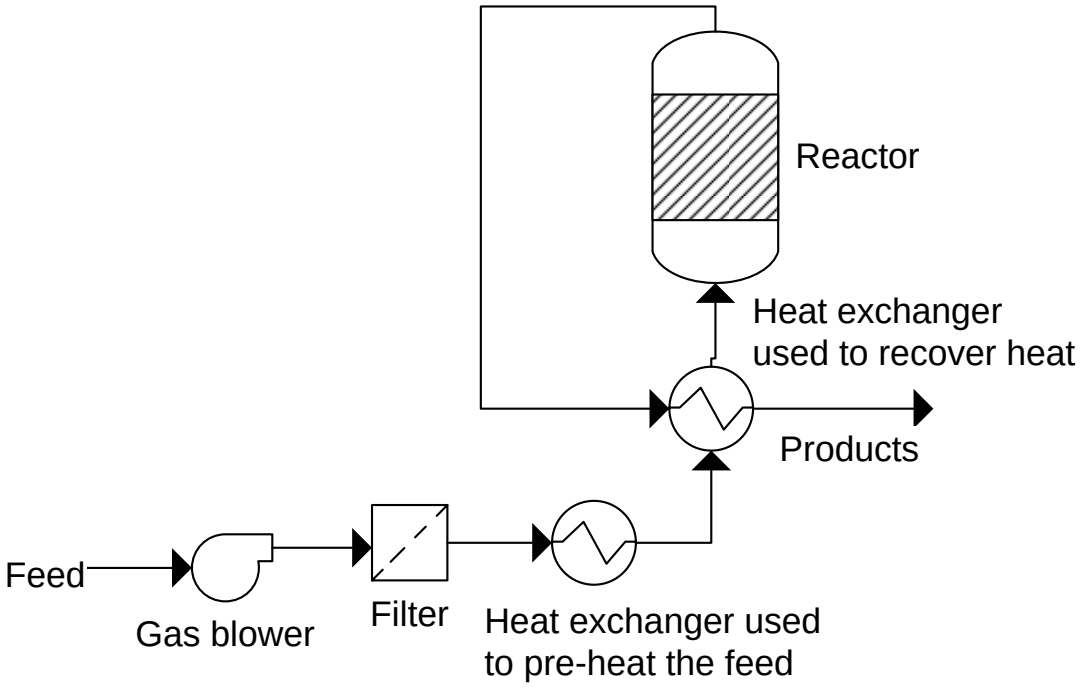
Reactor
Heat exchanger
used to recover heat
Products
Feed
Gas blower
Filter
Heat exchanger used
to pre-heat the feed

Figure 5

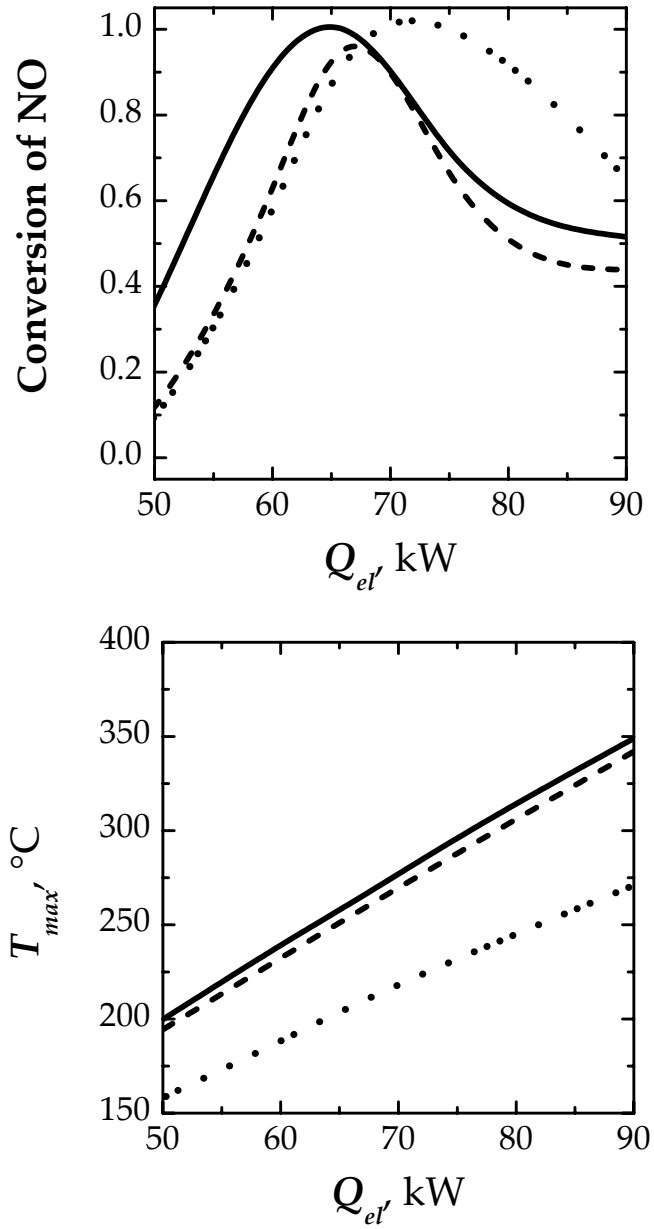
Conversion of NO
1.0
0.8
0.6
0.4
0.2
0.0
50
60
70
80
90
Q_{el}, kW
T_{max}, °C
400
350
300
250
200
150
50
60
70
80
90
Q_{el}, kW

Figure 6

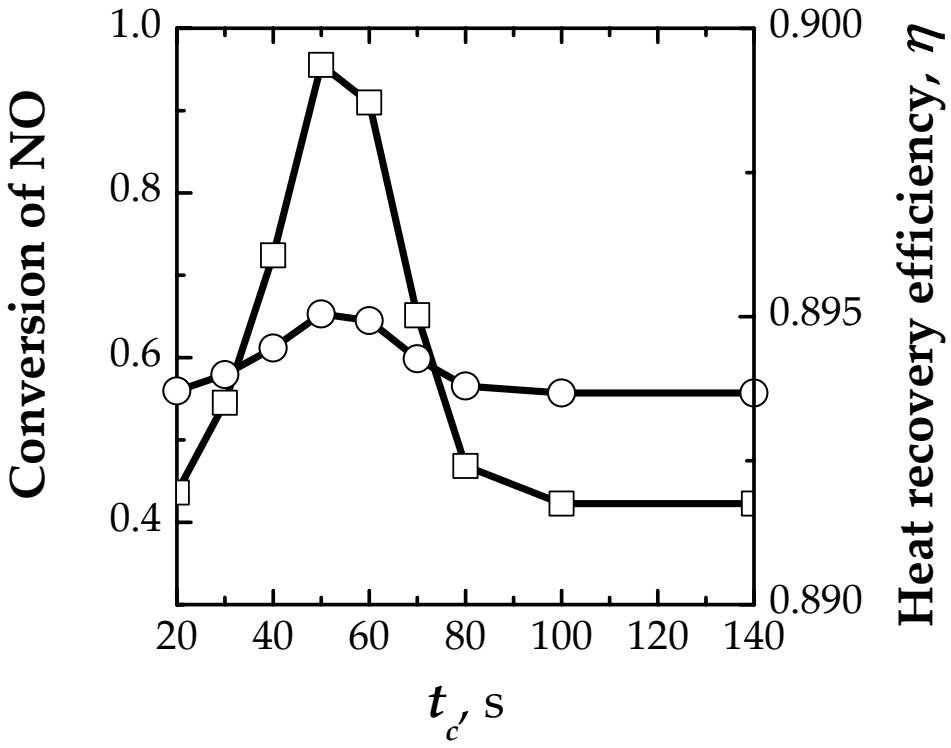
1.0
0.8
0.6
0.4
0.900
0.895
0.890
20
40
60
80
100
120
140
Conversion of NO
Heat recovery efficiency, η
t_c, s

Figure 7

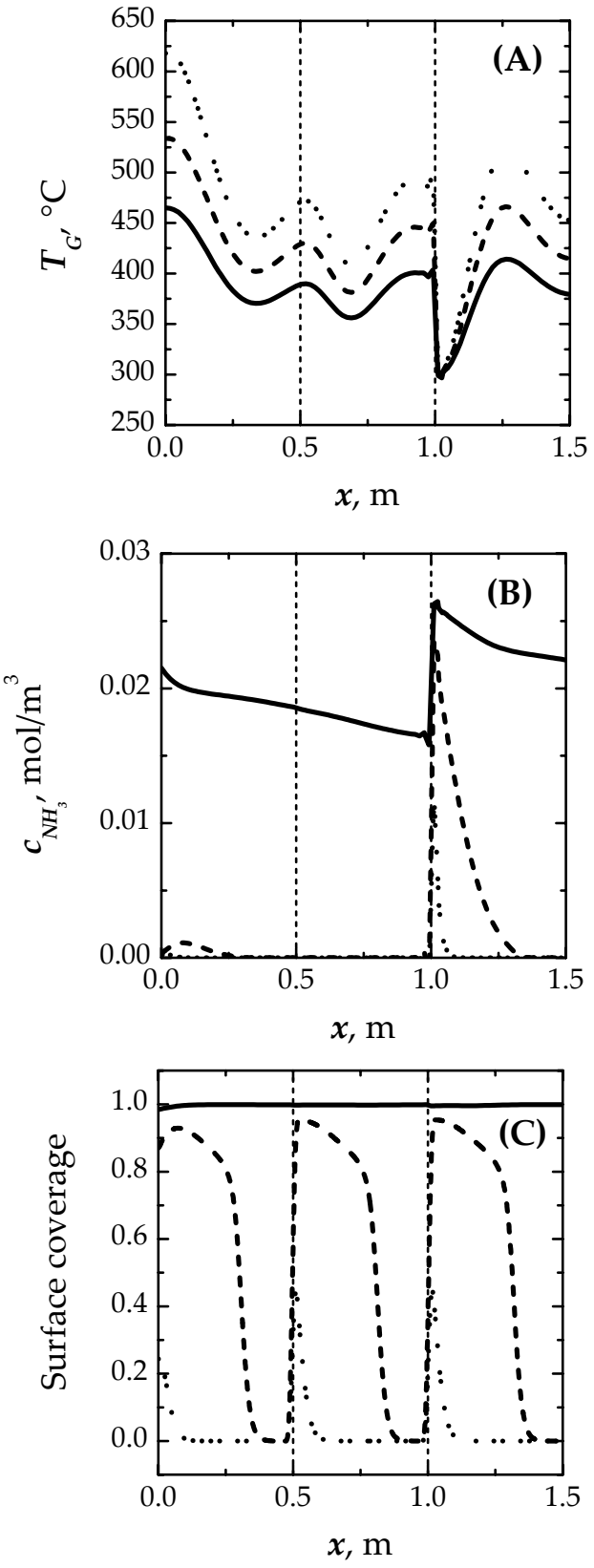
(A)
650
600
550
500
450
400
350
300
250
T_G, °C
0.0
0.5
1.0
1.5
x, m
(B)
0.03
0.02
0.01
0.00
c_{NH_3}, mol/m^3
0.0
0.5
1.0
1.5
x, m
(C)
1.0
0.8
0.6
0.4
0.2
0.0
Surface coverage
0.0
0.5
1.0
1.5
x, m

Figure 8

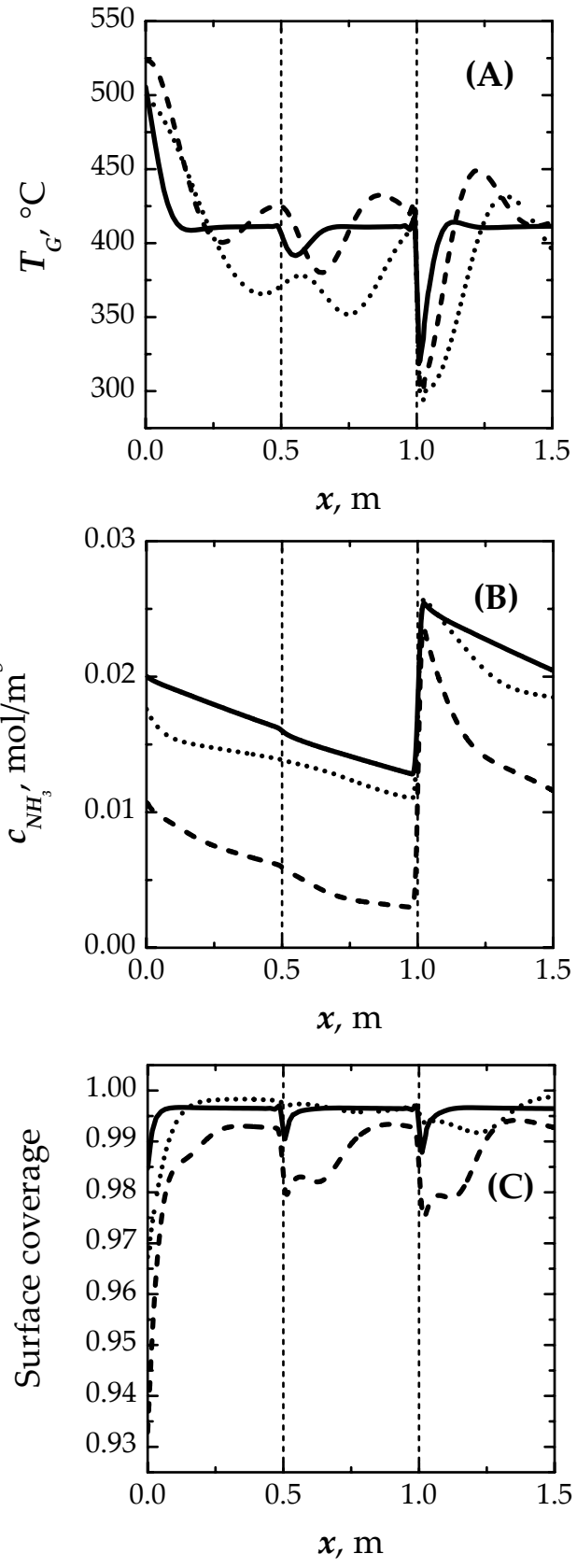
(A)
$T_{G'}$, °C
550
500
450
400
350
300
0.0
0.5
1.0
1.5
x, m
(B)
c_{NH_3}, mol/m^3
0.03
0.02
0.01
0.00
0.0
0.5
1.0
1.5
x, m
(C)
Surface coverage
1.00
0.99
0.98
0.97
0.96
0.95
0.94
0.93
0.0
0.5
1.0
1.5
x, m

Figure 9

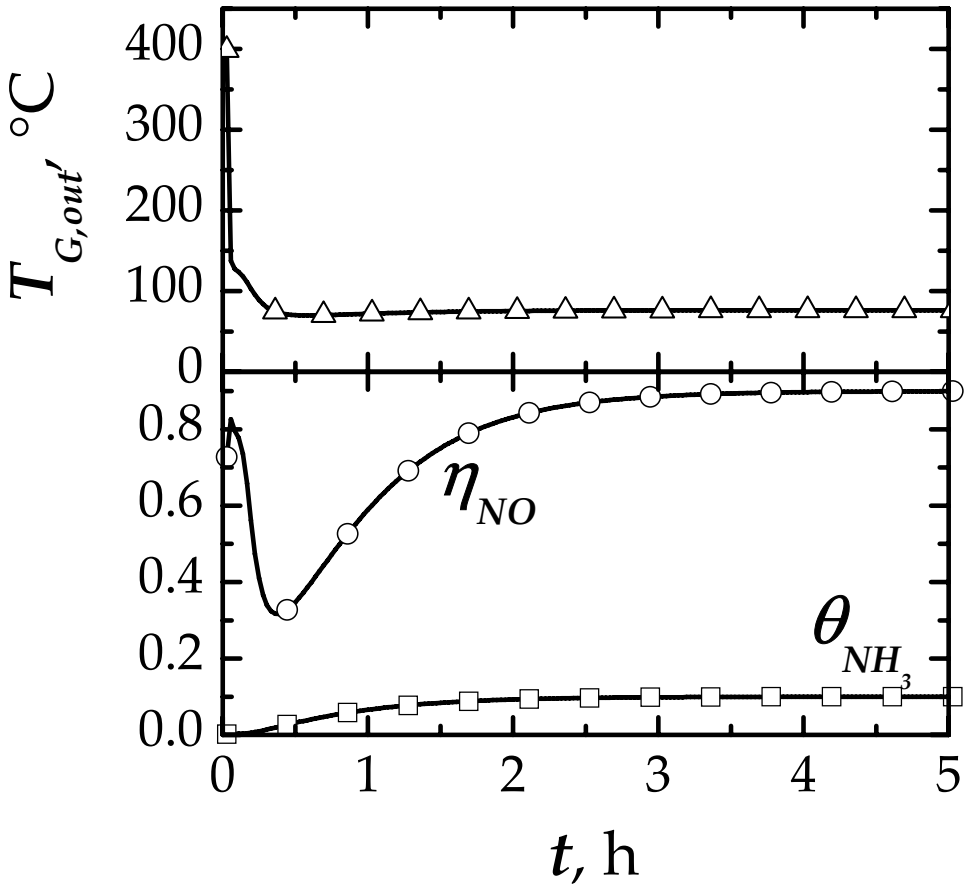
$T_{G,out'}$ °C
400
300
200
100
0
0.8
0.6
0.4
0.2
0.0
η_{NO}
θ_{NH_3}
0
1
2
3
4
5
t, h

Figure 10

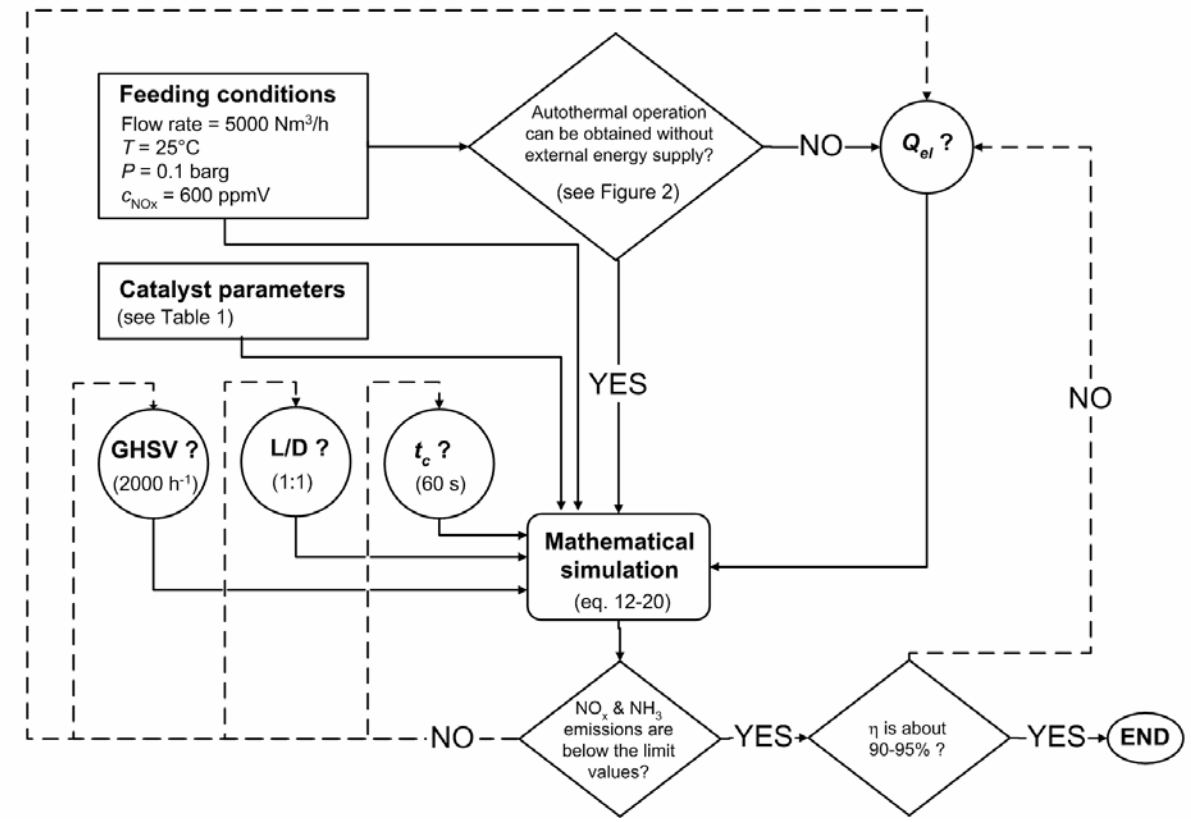
Feeding conditions
Flow rate = 5000 Nm³/h
T = 25°C
P = 0.1 barg
c_NOx = 600 ppmV
Autothermal operation can be obtained without external energy supply?
(see Figure 2)
NO
Q_el ?
Catalyst parameters
(see Table 1)
YES
NO
GHSV ?
(2000 h⁻¹)
L/D ?
(1:1)
t_c ?
(60 s)
Mathematical simulation
(eq. 12-20)
NO
NO_x & NH_3 emissions are below the limit values?
YES
η is about 90-95% ?
YES
END

Figure 11

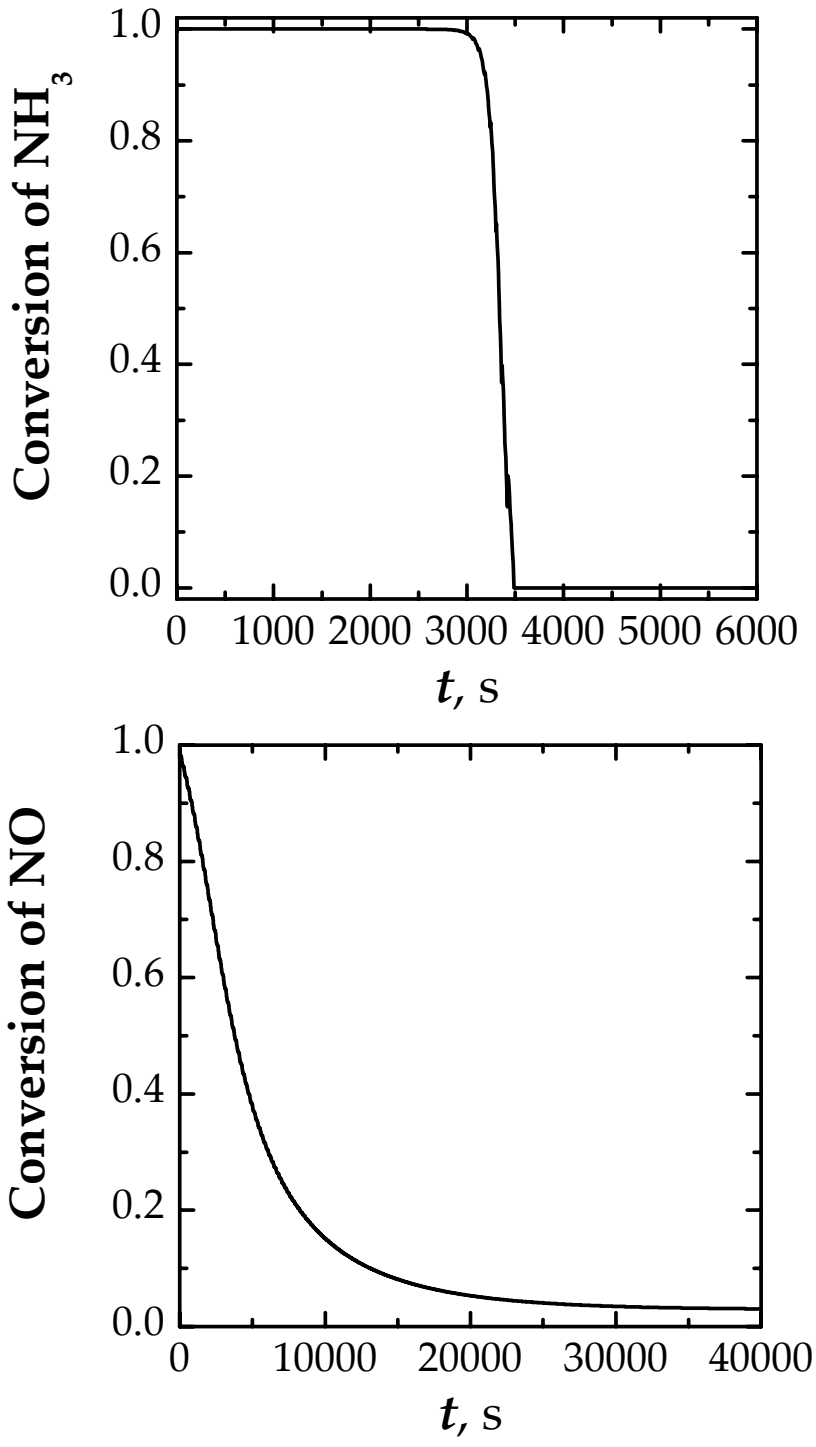
Conversion of NH3
1.0
0.8
0.6
0.4
0.2
0.0
0
1000
2000
3000
4000
5000
6000
t, s
Conversion of NO
1.0
0.8
0.6
0.4
0.2
0.0
0
10000
20000
30000
40000
t, s